Optical Materials 88 (2019) 630–634

Contents lists available at ScienceDirect

Optical Materials

journal homepage: www.elsevier.com/locate/optmat

Rhenium diselenide as the broadband saturable absorber for the nanosecond passively Q-switched thulium solid-state lasers

Shiqiang Wang[a], Haitao Huang[a,b,*], Xuan Liu[b], Haiwei Chen[a], Wei Zhou[a,b], Shande Liu[c], Deyuan Shen[a,b]

[a] School of Physics and Electronic Engineering, Jiangsu Key Laboratory of Advanced Laser Materials and Devices, Jiangsu Normal University, Xuzhou, 221116, China
[b] Jiangsu Collaborative Innovation Center of Advanced Laser Technology and Emerging Industry, Jiangsu Normal University, Xuzhou, 221116, China
[c] College of Electronics, Communication, and Physics, Shandong University of Science and Technology, Qingdao, 266590, China

ARTICLE INFO

Keywords:
Nanomaterials
Broadband saturable absorbers
Passively Q-switched
Tm-doped
Solid-state lasers

ABSTRACT

The feasibility of using rhenium diselenide ($ReSe_2$) as the saturable absorber for the broadband passively Q-switched (PQS) thulium solid-state lasers was demonstrated in this paper. In the short wavelength of 2 μm region, the combination of Tm:YLF and $ReSe_2$ was used to achieve the PQS operation with multi-wavelength around 1900 nm. A maximum average output power of 862 mw, a shortest pulse width of 527.9 ns and a repetition rate of 54 kHz were obtained. In the long wavelength of 2 μm region, a $ReSe_2$-based PQS multi-wavelength Tm:Y_2O_3 laser around 2050 nm was realized, generating a maximum average output power of 1.04 W, a shortest pulse width of 727 ns and a repetition rate of 106 kHz. The output performance of the $ReSe_2$-based pulsed laser is competitive among these PQS thulium solid-state lasers using the emerging two-dimensional materials as SAs, indicating that $ReSe_2$ is a promising broadband SA for the 2 μm solid-state lasers.

1. Introduction

The trivalent thulium ion (Tm^{3+}) doped laser sources operating at 2 μm are widely used in laser radar, laser medical treatment, remote sensing detection, atmospheric monitoring and organic material processing, and can also be used as pumping sources for 3 μm Cr^{2+} lasers and 3–5 μm optical parameter oscillators [1–3]. The most interesting transition of Tm^{3+} around 2 μm starts in the $^3F_4$ manifold of Tm^{3+} and ends in a thermally populated Stark level of the $^3H_6$ ground state. The doping-concentration-dependent cross-relaxation process in Tm^{3+} ions can support a high-slope-efficiency well beyond Stokes limit. Furthermore, Tm-doped laser materials have broadband absorption induced by the transition of $^3H_6 \rightarrow {}^3H_4$, which allows direct pumping of Tm^{3+} ions by ~800 nm AlGaAs laser diode (LD). These advantages make Tm solid-state lasers increasingly attractive in the 2 μm wavelength region. Sesquioxides have strong Stark splitting and low phonon energy that can result in broad emission spectra and high quantum efficiency. Furthermore, the high thermal conductivity of sesquioxides is considerably attractive for high power laser operations. Compared to single crystals, transparent ceramics attract much attention because they can be fabricated with large size, high dopant concentration and composite structure in much lower temperature environments. In addition, transparent ceramics not only have the optical and thermal properties that single crystals have, but also have better mechanical properties.

Developing new saturable absorbers (SAs) for Q-switched lasers and mode-locked lasers plays an important role in ultrafast photonics and related applications. In recent years, the two-dimensional (2D) materials represented by graphene, topological insulators, transition metal dichalcogenides (TMDs), and black phosphorus, have inspired considerable application as SAs for generating short pulses in solid-state and fiber lasers [4–6]. In comparison with conventional SAs, such as Cr:ZnSe and Cr:ZnS, these 2D materials as SAs have these advantages of controllable modulation depth, ultrafast recovery time, and broadband saturable absorption, as well as easy fabrications. Rhenium dichalcogenides (ReX_2, X = S or Se) are an emerging class of TMDs characterized by an unusually distorted octahedral (1T) crystal structure with triclinic symmetry. As a result of the distorted 1T structure, the bandgap of ReX_2 shows weak dependence on the layer number (1.35 eV for bulk and 1.43 eV for monolayer ReS_2 [7]; 1.26 eV for the bulk and 1.32 eV for monolayer $ReSe_2$ [8]). Su et al. have demonstrated that the impurities or defects in ReS_2 can result in the reduction of bandgap. Using ReS_2 as SA, passively Q-switched solid-state lasers at wavelengths of 0.64, 1.064, and 1.991 μm have been realized successfully [9]. As for the $ReSe_2$, the nonlinear saturable absorption characteristics and

* Corresponding author. School of Physics and Electronic Engineering, Jiangsu Key Laboratory of Advanced Laser Materials and Devices, Jiangsu Collaborative Innovation Center of Advanced Laser Technology and Emerging Industry, Jiangsu Normal University, Xuzhou, 221116, China.
E-mail address: hht840211@163.com (H. Huang).

https://doi.org/10.1016/j.optmat.2018.12.042
Received 3 December 2018; Received in revised form 27 December 2018; Accepted 28 December 2018
Available online 17 January 2019
0925-3467/

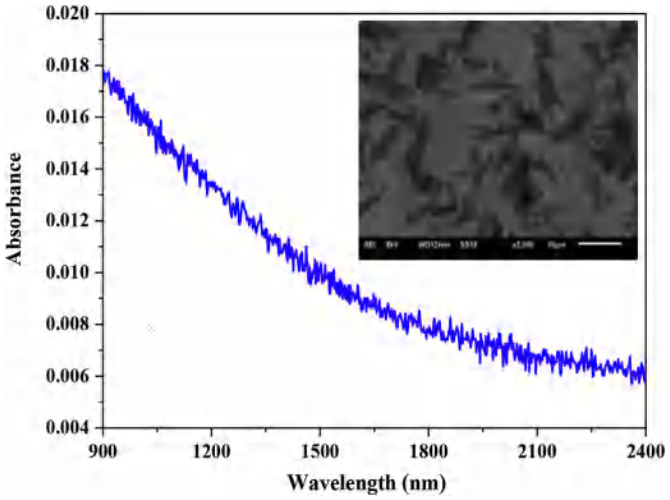

Fig. 1. The SEM and the absorption spectrum of the $ReSe_2$.

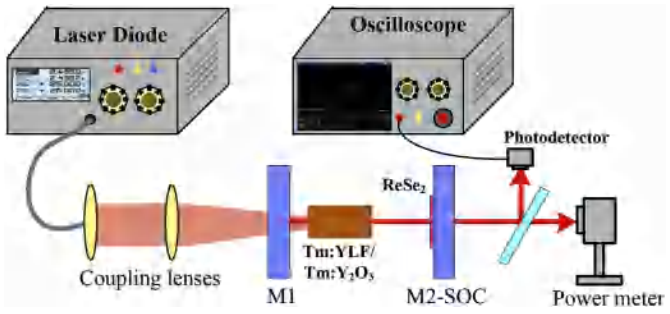

Fig. 2. Schematic diagram of the experimental setup for the $ReSe_2$-based passively Q-switched laser.

related experimental applications in short pulse generation have been rarely reported. Up to now, a passively Q-switched 1.55 μm Er fiber laser using $ReSe_2$ as SA has been achieved, outputting pulses with 36 nJ pulse energy and 4.98 μs pulse width [10]. The potential of using $ReSe_2$ to generate short pulse width and high pulse energy at other attractive wavelengths remain to be further developed.

In this paper, we experimentally demonstrated the nanosecond laser performance of $ReSe_2$ passively Q-switched Tm solid-state lasers with broadband multiple wavelengths covering the 1.87–2.05 μm. The $ReSe_2$ was directly deposited on one surface of the plano-plane output mirror, forming a compact configuration of saturable output coupler (SOC). With Tm:YLF crystal as gain medium, a high pulse energy PQS laser with multi-wavelength around 1900 nm was realized, corresponding to a maximum average output power of 862 mw, a shortest pulse width of 527.9 ns and a repetition rate of 54 kHz. For the longer wavelength, a $ReSe_2$-based PQS Tm:Y_2O_3 ceramic laser around 2050 nm was further reported, generating a maximum average output power of 1.04 W, a shortest pulse width of 727 ns and a repetition rate of 106 kHz. Our results indicated that $ReSe_2$ was a promising broadband SA for 2 μm solid-state lasers.

2. Material characterizations and experimental setup

High quality few-layered $ReSe_2$ SA was fabricated by using liquid phase exfoliation method. Firstly, $ReSe_2$ bulk with purity of 99.99% was ground into powder, then mixed those powder with alcohol and sonicated for 5 h to separate large-size sheets. Secondly, the as-prepared solution was centrifuged at 2500 rmp for 10 min, and the supernatant liquor was collected for standby. Finally, the processed $ReSe_2$ SA solution was prepared successfully.

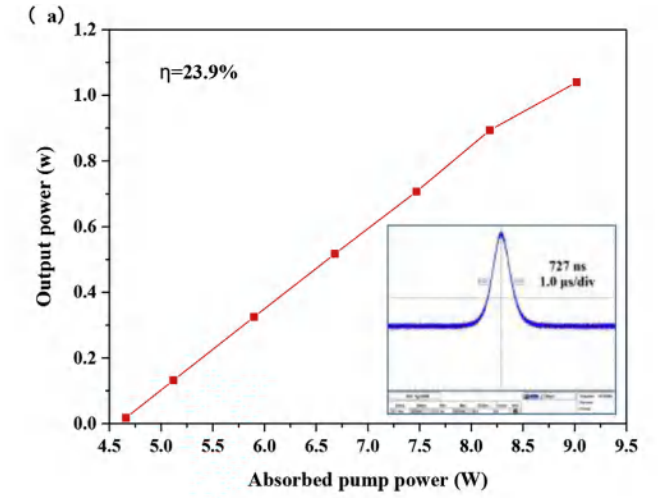

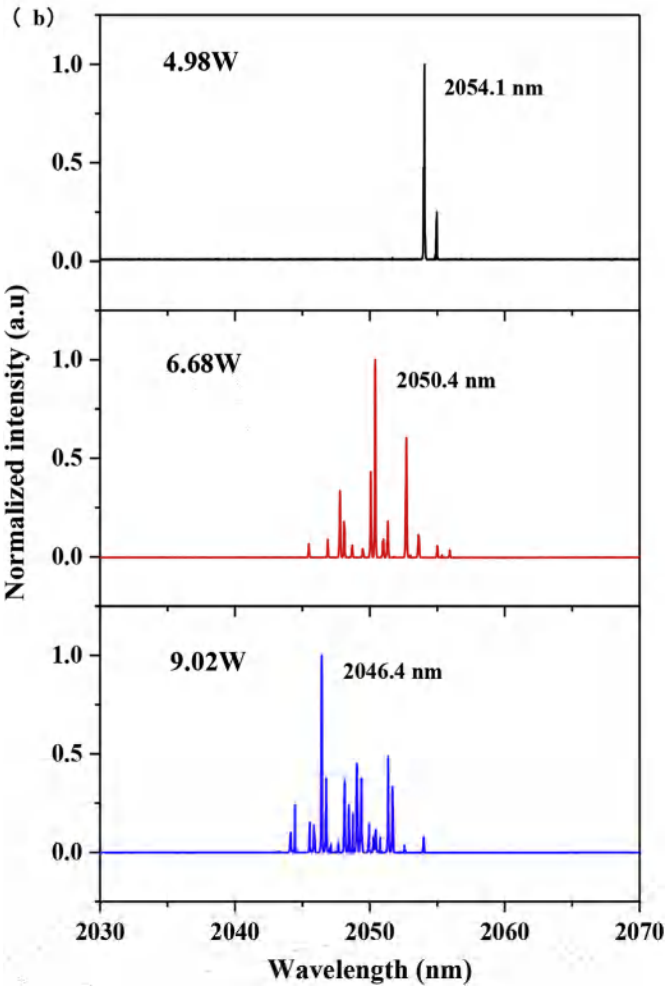

Fig. 3. (a) Average output power as a function of absorbed pump power with the inset showing the shortest pulse width of 727 ns and (b) oscillation wavelength under different absorbed power.

The scanning electron microscope (SEM) image of the fabricated $ReSe_2$ sample was measured by a JSM-6510 SEM (JEOL). Surface morphology of the $ReSe_2$ sample is shown in the inset of Fig. 1. Because liquid water shows strong absorption in the wavelength range of 1.4–2.1 μm, the absorption spectrum of $ReSe_2$ samples was measured with a non-solution-based sample [11]. The fabricated $ReSe_2$ SA

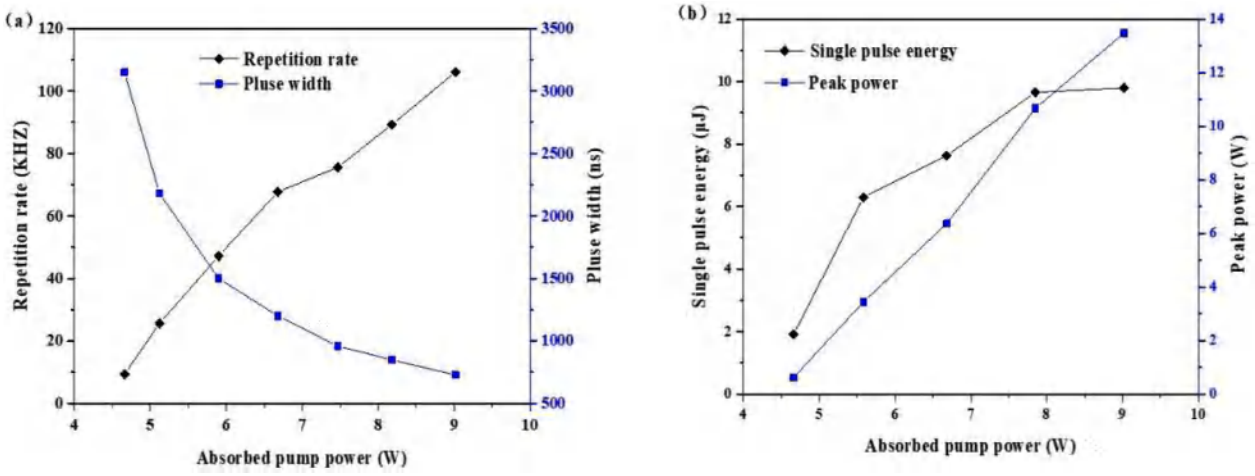

Fig. 4. (a) The pulse width and repetition rate versus the absorbed pump power and (b) the single pulse energy and pulse peak power versus absorbed pump power.

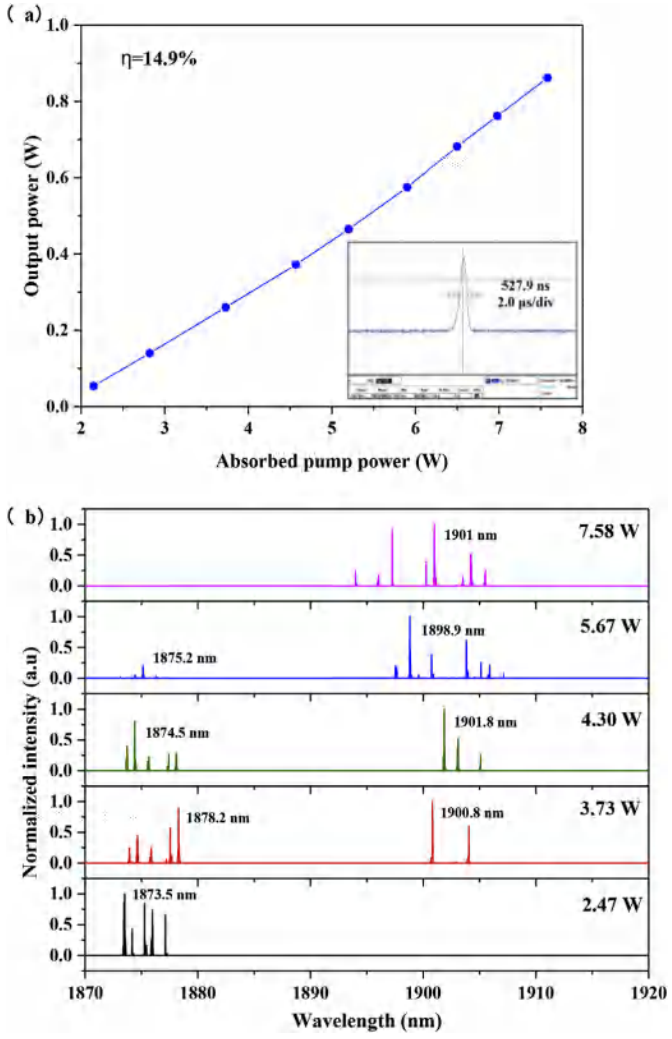

Fig. 5. (a). Output power versus absorbed pump power under PQS operation with the inset showing the shortest pulse width of 527.9 ns and (b) oscillation wavelength under different pump powers.

solution sample was dropped on a quartz glass substrate, followed by a slow drying at room temperature. The absorption spectrum of $ReSe_2$ was measured by a UV-VIS-NIR spectrophotometer (Lambda 950; Perkin-Elmer, Waltham, MA), ranging from 900 to 2400 nm, as shown by Fig. 1. It can be seen that the absorbance decreases at long wavelengths.

Different host materials provide the possibility to access a broadband wavelength ranging from 1.8 to 2.1 μm with the $^3F_4 \rightarrow {}^3H_6$ transition in Tm lasers. In order to evaluate the broadband saturable absorption of $ReSe_2$ for 2 μm Tm lasers, Tm:YLF and Tm:Y_2O_3 were chosen as the gain medium. Tm:YLF is characterized by a broadband structured emission spectra around 1900 nm, covering the short wavelength of 2 μm region. Tm:Y_2O_3 has a strong ground-level Stark splitting, enabling the emission spectrum extend to the longer wavelength of 2 μm region [12–14]. Furthermore, Tm:YLF has a longer upper-level lifetime of ~15 ms, and Tm:Y_2O_3 has a shorter upper-level lifetime of ~3.5 ms in comparison with the commonly used Tm-doped bulk laser materials. This direct comparison between the two combinations can extend the performance of $ReSe_2$ as SA in the Q-switched Tm lasers. The experimental arrangement for the $ReSe_2$-based Q-switching of a laser diode (LD) end-pumped Tm solid-state laser is shown schematically in Fig. 2. A linear cavity was employed for Q-switching laser experiments. The pump source was a fiber-coupled 785 nm LD, which had a core diameter of 400 μm and a numerical aperture of 0.22. Its radiation was coupled into the laser gain medium with a spot radius of 200 μm by a lens assembly.

The laser resonator used plane-plane configuration, which was composed of an input mirror M1, a Tm:Y_2O_3 ceramic or a Tm:YLF crystal, and a $ReSe_2$-based output coupler M2. M1 was a plano-plane mirror with high-transmission coatings at 785 nm (T > 98%) on one surface, high-reflection coatings at 1850–2100 nm (R > 99.8%) on the other surface. The Tm:Y_2O_3 transparent ceramic with 2 at.% Tm^{3+} doping concentration was both optically polished, and both ends of the ceramic were antireflection coated at 760–810 nm and 1950–2150 nm. The both ends of a a-cut 1.5 at.% Tm:YLF crystal with the size of $4 \times 4 \times 8\ mm^3$ long were antireflection coated at 795 nm and 1910 nm. For efficient thermal removal, gain mediums were wrapped by indium foil and mounted in a copper block with water cooled at 16 °C. The plano-plane mirror M2 was coated with T = 5% transmission at 1850–2100 nm. The $ReSe_2$ solution was deposited on the surface with partial-reflection coatings of the M2 output mirror, which served as the passive Q-switcher, followed by a slow drying at room temperature. This SOC configuration makes the laser resonator more compact (only 20 mm long) and reduces insertion loss. The initial transmittance of M2 deposited with $ReSe_2$ was measured to be about 2.3% at 2000 nm.

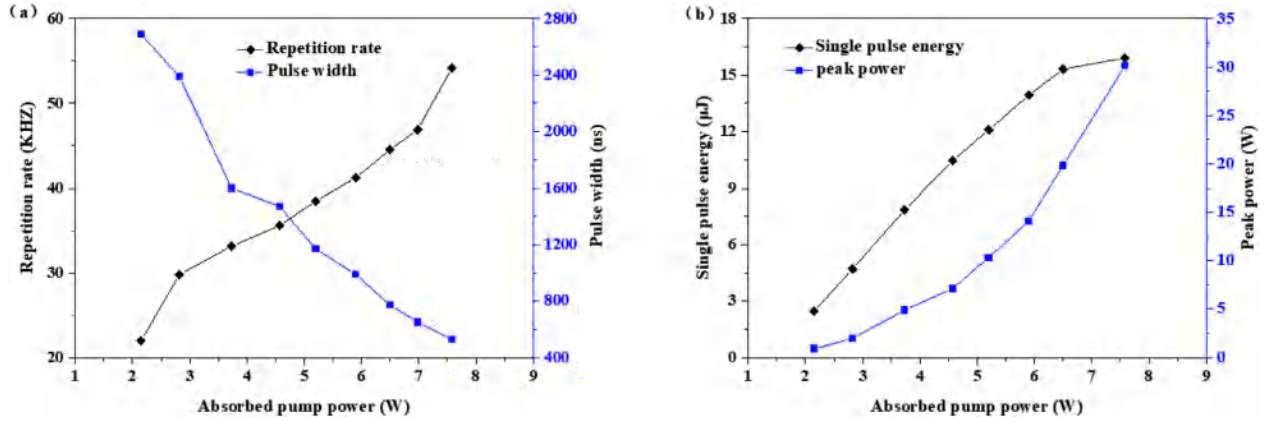

Fig. 6. (a) The pulse width and repetition rate versus the absorbed pump power and (b) the single pulse energy and pulse peak power versus absorbed pump power.

Table 1
Summary of passively Q-switched Tm solid-state 2 μm lasers based on promising 2D SAs.

Gain medium	SA	Pulse width	Repetition rate	Average output power	Single pulse energy	Peak power	Ref
		ns	kHz	W	μJ	W	
Tm: LuAG	WS_2	660	63	1.08	17	26	[4]
Tm:YAP	$MoTe_2$	380	144	1.21	8.4	22.2	[15]
Tm,Ho:YAP	MoS_2	435	55	0.27	5	11.3	[16]
Tm:YAP	ReS_2	415	677	0.245	0.36	8.72	[9]
Tm:YAG	BP	3120	11.6	0.0385	3.32	–	[17]
$Tm:CaYAlO_4$	MoS_2	480	102.6	0.49	4.87	9.2	[18]
Tm:LuAG	$MoSe_2$	520	158	1.19	12.7	21.8	[19]
Tm:YAP	Graphene	735	42.4	0.362	8.5	–	[20]
Tm:YAG	Bi_2Te_3	382	57.67	0.272	4.8	12	[21]
Tm:YLF	Graphene Oxide	1038	38.33	0.379	9.89	9.53	[22]
$Tm:Y_2O_3$	$ReSe_2$	727	106	1.04	9.81	13.49	This work
Tm:YLF	$ReSe_2$	527.9	54	0.862	15.96	30.23	This work

"-" means no relevant data.

3. Experimental results and discussions

3.1. $Tm:Y_2O_3$ laser

By inserting the $ReSe_2$-deposited M2 into the cavity, typical passive Q-switching operations with different gain mediums were realized under a wide range of absorbed pump powers. The absorbed pump power was measured under lasing conditions as follows. The pump power transmitted through the input mirror M1 was first measured, which was denoted as the incident pump power. Then the residual pump light passing through the output coupler M2 was separated from the laser radiation by a bandpass filter. Further considering the partial reflection by the output coupler, the pump absorption efficiency under lasing conditions was determined to be 45% for $Tm:Y_2O_3$ and 38% for Tm:YLF, respectively. For the $Tm:Y_2O_3$ ceramic PQS laser operation, the dependence of the output power on the absorbed pump power is shown in Fig. 3a. Under the absorbed pump power of 9.02 W, the maximum output power was 1.04 W, corresponding to a slope efficiency of 23.9%, respectively. The M^2 factor of the beam was measured to be around 3.5. Laser output spectrums at different absorption pump powers were measured with an optical spectrum analyzer (Yokogawa, AQ6375), as shown in Fig. 3b. The $ReSe_2$ passively Q-switched $Tm:Y_2O_3$ laser operated in a multi-wavelength state around 2050 nm, which was the same as in the continuous state. Under a low absorbed pump power of 4.98 W, the peak of lasing wavelength was located in 2054.1 nm. When the absorbed pump power was increased to 6.68 W, multiple emission peaks began to oscillate and were found blue-shifted. Under the maximum output power of 1.04 W, corresponding to the absorbed pump power of 9.02 W, multiple emission peaks further moved toward short wavelength direction. We attributed the wavelength blue shift to the reduction of the reabsorption effect that came with the depopulation of the ground-state level under the Q-switching process. The oscillating modes are increased with the pump power, whichs result from the change of inversion ratio that came with the change of pump power.

The pulse width and pulse repetition rate versus the absorbed pump power is shown in Fig. 4a. The pulse duration was shortened from 3.15 μs to 727 ns with an increase of absorbed pump power from 4.66 W to 9.02 W, while the pulse repetition rate increased almost linearly from 9.34 kHz to 106 kHz. The calculated single pulse energy and peak power versus the absorbed pump power is shown in Fig. 4b. The maximum single pulse energy was calculated as 9.81 μJ, corresponding to the maximum pulse peak power of 13.49 W.

3.2. Tm:YLF

For the Tm:YLF crystal PQS laser experiment, as shown in Fig. 5a, a maximum average output power of 862 mW was obtained under the absorped pump power of 7.58 W, corresponding to a slope efficiency of 14.9%. The beam quality of the output laser was relatively stable with the increase of pump power, the M^2 factor of the beam was measured to be around 1.1. With the increasing of absorbed pump power, the laser output spectrums changed accordingly, as shown in Fig. 5b. The $ReSe_2$ passively Q-switched Tm:YLF crystal laser also operated in a multi-wavelength state. Under a low absorbed pump power of 2.47 W, the peak laser output spectrum was located in 1873.5 nm. When the absorbed pump power was increased to 3.73 W, the lasing wavelength around 1900 nm began to appear. With the increase of absorbed pump power, the intensity of wavelength around 1875 nm gradually weakened, while the intensity of wavelength around 1900 nm increased

accordingly. When the absorbed pump power was increased to 5.67 W, the intensity of the 1875 nm band became very weak. With the absorbed pump power continuing to be increased, the 1875 nm band disappeared completely. Under the maximum output power of 862 mW, corresponding to the absorbed pump power of 7.58 W, the laser output wavelength was only located around 1901 nm. Compared with the continuous state, the output spectrum around 1875 nm appeared under the Q-switched state. The increased inversion population density induced by the Q-switching gave the multi-wavelengths an opportunity to oscillate simultaneously.

The relationship of the pulse width and repetition rate versus the absorbed pump power is shown in Fig. 6a. With the increase in repetition rate from 22 kHZ to 54 kHZ, the pulse width decreased from 2.69 μs to 527.9 ns. The shortest pulse width of 527.9 ns is smaller than obtained in the Q-switched Tm:Y_2O_3 ceramic laser. Fig. 6b shows the calculated single pulse energy and peak power versus the absorbed pump power. The maximum single pulse energy was calculated as 15.96 μJ, corresponding to the maximum pulse peak power of 30.23 W. Compared with the Tm:Y_2O_3 laser operation, both the pulse width and pulse repetition rate are considerably reduced in the case of Tm:YLF, resulting in the increased single pulse energy and peak power. This improved performance can be attributed to the fact that Tm:YLF has a longer upper level lifetime than that of Tm:Y_2O_3. Longer upper-level lifetime can offer an increased energy storage capability, producing enough inversion population accumulation to generate Q-switched pulses with low repetition rates. So the initial inversion population can be fully consumed during the interval when the Q-switch is turned on, the rise time of a pulse will be reduced. Then, the pulses with short pulse width are generated.

Table 1 gives a comparison of the performance of the passively Q-switched Tm solid-state lasers based on 2D-material SAs in the 2 μm region. The output performance of the $ReSe_2$-based pulsed laser is competitive among these PQS lasers. For the $ReSe_2$-based Tm:YLF PQS laser, the peak power of 30.23 W and the single pulse energy of 15.96 μJ stand out from these PQS Tm solid-states lasers. Furthermore, the combination of $ReSe_2$ and Tm:Y_2O_3 also provides a new way for generating nanosecond laser pulses in the longer wavelength of 2 μm region, which can be a cost-effective alternative to Ho-doped lasers.

4. Conclusions

In conclusion, the experimental results demonstrated the possibility of generating nanosecond pulses by using $ReSe_2$ as SA in Tm solid-state lasers with wavelength from 1.87 to 2.05 μm. The $ReSe_2$-based output mirror combining the function of passive Q-switching and output coupling was used in our experiments. With Tm:YLF crystal as gain medium, a high pulse energy pulsed laser emitting multiple wavelengths around 1900 nm was demonstrated. For the longer wavelength, a $ReSe_2$-based PQS multi-wavelength Tm:Y_2O_3 ceramic laser around 2050 nm was reported. Our work indicates that the novel $ReSe_2$ is a promising broadband saturable absorber for nanosecond Q-switched lasers in the 2 μm wavelength region.

Declaration of interests

None.

Acknowledgments

This work is supported by the National Natural Science Foundation of China (61875077, 61605068 and 61805111), Applied Basic Research Programs of Xuzhou (KC17085), the Natural Science Foundation of the Jiangsu Higher Education Institutions of China (18KJA510001), and the Priority Academic Program Development of Jiangsu Higher Education Institutions (PAPD).

References

[1] K. Scholle, S. Lamrini, P. Koopmann, P. Fuhrberg, 2 μm laser sources and their possible applications, in: B. Pal (Ed.), Frontiers in Guided Wave Optics and Optoelectronics, Intech, 2010.
[2] B. Cole, L. Goldberg, S. Chinn, L.A. Pomeranz, K.T. Zawilski, P.G. Schunemann, J. McCarthy, Compact and efficient mid-IR OPO source pumped by a passively Q-switched Tm:YAP laser, Opt. Lett. 43 (2018) 1099–1102.
[3] O.L. Antipov, I.D. Eranov, M.P. Frolov, Y.V. Korostelin, V.I. Kozlovsky, A.A. Novikov, Y.P. Podmar'kov, Y.K. Skasyrsky, 2.92 μm Cr^{2+}:CdSe single crystal laser pumped by a repetitively pulsed Tm^{3+}:Lu_2O_3 ceramics laser at 2.066 μm, Laser Phys. Lett. 12 (2015) 045801.
[4] C. Luan, K. Yang, J. Zhao, S. Zhao, L. Song, T. Li, H. Chu, J. Qiao, C. Wang, Z. Li, S. Jiang, B. Man, L. Zheng, WS_2 as a saturable absorber for Q-switched 2 micron lasers, Opt. Lett. 41 (2016) 3783–3786.
[5] H.K. Zhang, J.L. He, Z.W. Wang, J. Hou, B.T. Zhang, R.W. Zhao, K.Z. Han, K.J. Yang, H.K. Nie, X.L. Sun, Dual-wavelength passively Q-switched Tm:YAP laser with black phosphorus saturable absorber, Opt. Mater. Express 6 (2016) 2328–2335.
[6] Z. You, Y. Sun, D. Sun, Z. Zhu, Y. Wang, J. Li, C. Tu, J. Xu, High performance of a passively Q-switched mid-infrared laser with Bi_2Te_3/graphene composite SA, Opt. Lett. 42 (2017) 871–874.
[7] E. Liu, Y. Fu, Y. Wang, Y. Feng, H. Liu, X. Wan, W. Zhou, B. Wang, L. Shao, C.H. Ho, Y.S. Huang, Z. Cao, L. Wang, A. Li, J. Zeng, F. Song, X. Wang, Y. Shi, H. Yuan, H.Y. Hwang, Y. Cui, F. Miao, D. Xing, Integrated digital inverters based on two-dimensional anisotropic ReS_2 field-effect transistors, Nat. Commun. 6 (2015) 6991.
[8] H. Zhao, J. Wu, H. Zhong, Q. Guo, X. Wang, F. Xia, L. Yang, P. Tan, H. Wang, Interlayer interactions in anisotropic atomically thin rhenium diselenide, Nano Res 8 (2015) 3651–3661.
[9] X.C. Su, B.T. Zhang, Y. Wang, G.B. He, G. Li, N. Lin, K.J. Yang, J.L. He, S.D. Liu, Broadband rhenium disulfide optical modulator for solid-state lasers, Photon. Res. 6 (2018) 498–505.
[10] L. Du, G.B. Jiang, L.L. Miao, B. Huang, J. Yi, C.J. Zhao, S.C. Wen, Few-layer rhenium diselenide: an ambient-stable nonlinear optical modulator, Opt. Mater. Express 8 (2018) 926.
[11] H.T. Huang, M. Li, P. Liu, L. Jin, H. Wang, D.Y. Shen, Gold nanorods as the saturable absorber for a diode pumped nanosecond Q-switched 2 μm solid-state laser, Opt. Lett. 41 (2016) 2700–2703.
[12] H. Wang, H.T. Huang, P. Liu, L. Jin, D.Y. Shen, J. Zhang, D.Y. Tang, Diode-pumped continuous-wave and Q-switched Tm:Y_2O_3 ceramic laser around 2050 nm, Opt. Mater. Express 7 (2017) 296–303.
[13] P.A. Ryabochkina, A.N. Chabushkin, Y.L. Kopylov, V.V. Balashov, K.V. Lopukhin, Two-micron lasing in diode-pumped Tm: Y_2O_3 ceramics, Quant. Electron. 46 (2016) 597–600.
[14] H.T. Huang, H. Wang, D.Y. Shen, VBG-locked continuous-wave and passively Q-switched Tm:Y_2O_3 ceramic laser at 2.1 μm, Opt. Mater. Express 7 (2017) 3147–3154.
[15] B.Z. Yan, B.T. Zhang, H.K. Nie, H.Y. Wang, G.R. Li, X.L. Sun, R.H. Wang, N. Lin, J.L. He, High-power passively Q-switched 2.0 μm all-solid-state laser based on a $MoTe_2$ saturable absorber, Optic Express 26 (2018) 18505–18512.
[16] C. Luan, X.Y. Zhang, K.J. Yang, J. Zhao, S.Z. Zhao, T. Li, W.C. Qiao, H.W. Chu, J.P. Qiao, J. Wang, L.H. Zheng, X.D. Xu, J. Xu, High-peak power passively Q-switched 2 μm laser with MoS_2 saturable absorber, IEEE J. Sel. Top. Quant. Electron. 23 (2016) 1–5.
[17] G.Q. Xie, Black phosphorus-based saturable absorber for Q-switched Tm:YAG ceramic laser, Opt. Eng. 55 (2016) 081307.
[18] J.L. Lan, X.Y. Zhang, Z.Y. Zhou, B. Xu, H.Y. Xu, Z.P. Cai, N. Chen, J. Wang, X.D. Xu, R. Soulard, R. Moncorgé, Passively Q-switched Tm:$CaYAlO_4$ laser using a MoS_2 saturable absorber, IEEE Photon. Technol. Lett. 29 (2017) 15.
[19] X.Y. Liu, K.J. Yang, S.Z. Zhao, M. Li, W.C. Qiao, T. Li, S.Y. Zhang, L.H. Zheng, L.B. Su, J. Xu, J.T. Bian, High repetition rate all-solid-state pulsed 2 μm laser based on selenide molybdenum saturable absorber, IEEE J. Sel. Top. Quant. Electron. 24 (2017) 1600306.
[20] J. Hou, B.T. Zhang, J.L. He, Z.W. Wang, F. Lou, J. Ning, R.W. Zhao, X.C. Su, Passively Q-switched 2 μm Tm:YAP laser based on graphene saturable absorber mirror, Appl. Opt. 53 (2014) 4968.
[21] P. Gao, H.Z. Huang, X.H. Wang, H.G. Liu, J.H. Huang, W. Weng, S.T. Dai, J.H. Li, W.X. Lin, Passively Q-switched solid-state Tm:YAG laser using topological insulator Bi_2Te_3 as a saturable absorber, Appl. Opt. 57 (2018) 2020–2024.
[22] Y.Q. Zu, C. Zhang, Y.J. Wu, J.J. Liu, J. Liu, Y.G. Wang, Graphene oxide for diode-pumped Tm:YLF passively Q-switched laser at 2 μm, Chin. Optic Lett. 16 (2018) 020013.